

1995
11-20-10
OSIT
6-17
P-41

FINAL REPORT
ANALYSIS OF ADVANCED SOLID ROCKET MOTOR
IGNITION PHENOMENA

by

Winfred A. Foster, Jr.
Associate Professor

Rhonald M. Jenkins
Associate Professor

Prepared under

NASA Grant No. NAG8-923

between

George C. Marshall Space Flight Center
National Aeronautics and Space Administration

and

Auburn University
Engineering Experiment Station
Auburn University, Alabama 36849

July 25, 1995

(NASA-CR-199427) ANALYSIS OF
ADVANCED SOLID ROCKET MOTOR
IGNITION PHENOMENA Final Report
(Auburn Univ.) 41 p

N96-11221

Unclas

G3/20 0067497

ANALYSIS OF ADVANCED SOLID ROCKET MOTOR
IGNITION PHENOMENA

Winfred A. Foster, Jr. and Rhonald M. Jenkins

ABSTRACT

This report presents the results obtained from an experimental analysis of the flow field in the slots of the star grain section in the head-end of the advanced solid rocket motor during the ignition transient. This work represents an extension of the previous tests and analysis to include the effects of using a center port in conjunction with multiple canted igniter ports. The flow field measurements include oil smear data on the star slot walls, pressure and heat transfer coefficient measurements on the star slot walls and velocity measurements in the star slot.

ACKNOWLEDGEMENTS

The authors express appreciation to personnel of the George C. Marshall Space Flight Center (MSFC) for their support and assistance in this project. In particular, Mr. John E. Hengel, whose overall support of this project was an essential factor in its overall success and to Mr. Andrew W. Smith for his technical assistance. The authors also wish to thank to Mr. Billy H. Holbrook for his work in constructing the experimental models.

TABLE OF CONTENTS

ABSTRACTii

ACKNOWLEDGEMENTSiii

LIST OF FIGURESv

LIST OF TABLESvi

I. INTRODUCTIONI-1

II. EXPERIMENTAL ANALYSISII-1

 Experimental Apparatus.....II-2

 Test Facility.....II-7

 Test Plan.....II-9

 Oil Smear Results.....II-12

 Results From Static Pressure Measurements.....II-12

 Results From Heat Transfer Measurements.....II-12

 LDV Experiment.....II-28

 References.....II-33

LIST OF FIGURES

<u>FIG.</u>	<u>TITLE</u>	<u>PAGE NO.</u>
II-1	Schematic of star slot.....	II-4
II-2	Cross-section of star slot region.....	II-4
II-3	Schematic of head-end section.....	II-5
II-4	Head-end slots and igniter models.....	II-6
II-5	Location of pressure taps and calorimeters.....	II-8
II-6	Detail of calorimeter installation.....	II-8
II-7	Igniter 4 (100 psi).....	II-10
II-8	Igniter 5 (100 psi).....	II-10
II-9	Igniter 4 (1800 psi).....	II-11
II-10	Igniter 5 (1800 psi).....	II-11
II-11	Igniter 4 (100 psi).....	II-13
II-12	Igniter 5 (100 psi).....	II-13
II-13	Igniter 4 (500 psi).....	II-14
II-14	Igniter 5 (500 psi).....	II-14
II-15	Igniter 4 (1000 psi).....	II-15
II-16	Igniter 5 (1000 psi).....	II-15
II-17	Igniter 4 (1500 psi).....	II-16
II-18	Igniter 5 (1500 psi).....	II-16
II-19	Igniter 4 (1800 psi).....	II-17
II-20	Igniter 5 (1800 psi).....	II-17
II-21	Igniter 4 (100 psi).....	II-18
II-22	Igniter 5 (100 psi).....	II-18
II-23	Igniter 4 (500 psi).....	II-19
II-24	Igniter 5 (500 psi).....	II-19
II-25	Igniter 4 (1000 psi).....	II-20
II-26	Igniter 5 (1000 psi).....	II-20
II-27	Igniter 4 (1500 psi).....	II-21
II-28	Igniter 5 (1500 psi).....	II-21
II-29	Igniter 4 (1800 psi).....	II-22
II-30	Igniter 5 (1800 psi).....	II-22
II-31	Igniter 4 (100 psi).....	II-23
II-32	Igniter 5 (100 psi).....	II-23
II-33	Igniter 4 (500 psi).....	II-24
II-34	Igniter 5 (500 psi).....	II-24
II-35	Igniter 4 (1000 si).....	II-25
II-36	Igniter 5 (1000 psi).....	II-25
II-37	Igniter 4 (1500 psi).....	II-26
II-38	Igniter 5 (1500 psi).....	II-26
II-39	Igniter 4 (1800 psi).....	II-27
II-40	Igniter 5 (1800 psi).....	II-27
II-41	LDV experimental setup.....	II-29
II-42	LDV system in operation.....	II-30
II-43	Igniter models used for LDV measurements.....	II-31
II-44	Etching formed by Al particles on plexiglas slot..	II-32

LIST OF TABLES

<u>Table</u>	<u>Title</u>	<u>PAGE NO.</u>
II-1	Test matrix.....	II-9

I. INTRODUCTION

This report describes the results obtained from experimental analyses conducted for the purpose of evaluating the flow field characteristics in a star slot during the ignition phase of a solid rocket motor firing. In particular, this work focused on the flow fields induced in a star slot when an igniter is used which has both a centerport nozzle and multiple canted nozzles. This configuration was of interest because of its intended use on the Advanced Solid Rocket Motor (ASRM). The ASRM was a proposed replacement for the solid rocket booster currently in use on the Space Shuttle. This report describes the analyses done to evaluate the flow field characteristics. Although, the ASRM program was canceled after the present work was complete, the results described in this report are applicable to a general class of canted multiport igniters.

Section II presents the results of a series of experiments conducted at NASA's George C. Marshall Space Flight Center (MSFC). These experiments utilized a model designed and constructed in the Aerospace Engineering Department at Auburn University. This model is a one-tenth scale simulation of the Space Shuttle Redesigned Solid Rocket Motor (RSRM) head-end section. The model was originally built for flow field studies in the RSRM head end star.¹ These studies were directed at evaluating not only the flow field characteristics in the slot, but also, the differences between single port and canted multiport igniters. Because of time and cost constraints the RSRM star slot model geometry used previously was also used for the current study. There are differences between the RSRM and ASRM star slots. However, it is believed that the geometric differences between the slots would not substantially change the basic flow field characteristics being evaluated. Furthermore, the use of the same slot geometry provides a consistent basis for comparing the effects of an igniter with both a centerport nozzle and multiple canted nozzles to those with either a single centerport or with only canted multi-ports.

The model was tested in the special test section of the 14"x14" trisonic wind tunnel at MSFC. The tests were cold-flow, using air, simulations of the internal flow through the igniter nozzle and the head-end section of the SRM. The air was supplied through a special high pressure line connected to the wind tunnel. There was no external flow around the model. The tests were designed to provide both qualitative and quantitative data on the interaction between the igniter plume and the star slots and the flow field within the star slots. Qualitative measurements were made using oil smears, Schlieren photography and by seeding the flow field with aluminum particles which were illuminated with a laser system and recorded on video tape. Quantitative measurements were made of the pressure distribution

within a slot, the heat transfer rates to the wall of a slot and the flow velocity within the slot using an LDV system.

The correlation of the data between the various experiments performed is excellent.

The experimental database which has been generated from this work provides significant new insight into flow field phenomena occurring in the star slots of SRM's which have head-end star grains and head-end igniters.

II. EXPERIMENTAL ANALYSIS

One of the primary limitations of existing ignition transient prediction computer codes is an overestimation of the ignition delay and the departure of the predicted pressure-time history curve from measured data in the early part of the transient. One of the reasons for this is the lack of data on the flow field in star grain sections of solid rocket motors. The experiments described in this section focused on the flow field in the star grain section of the proposed Advanced Solid Rocket Motor. The purpose of the experiments was to obtain a credible data base for the flow field patterns and heat transfer rates within the star slots. A one-tenth scale model of the Space Shuttle RSRM head-end star grain was available from a previous study¹. The availability of experimental flow field data during the ignition transient in solid rocket motors is very scarce. Conover² conducted cold flow tests using a one-tenth scale model of the Space Shuttle solid rocket motor's head-end star grain section. Conover's tests used both a single port igniter, such as found on the RSRM and a three port igniter. That series of tests included Schlieren photographs of the igniter mounted in a plenum, oil smear data, pressure data and heat transfer coefficient measurements. Fifteen pressure ports were fitted in one side plate of a slot, while fifteen calorimeters to measure heat transfer coefficients were located in another slot. The data were taken at pressure levels from 100 to 1500 psi in 100 psi increments. The actual Space Shuttle igniter operates at approximately 2000 psi. Limits on the test facility prevented taking data at higher igniter chamber pressures. The static pressure data obtained provide some qualitative trends, but there was considerable scatter in the data when the igniter chamber pressure exceeded 1100 psi. This was probably due to the fact, as Conover states, that "above this pressure the side plates used to form the star grain slots were deflected to produce a one-sixteenth-inch gap where the plates come together at the star points," thus causing some leakage. There were also some apparent inconsistencies in the temperature data due to model warm-up during the test. However, the oil smear data provide a good indication of the recirculating flow pattern inside a slot. Even though Conover's experimental data provide useful information on the flow field inside the star slot, they should be considered preliminary in nature, and a starting point for a more in-depth investigation. Reference 1 provides considerably more data regarding the flow field characteristics in a star slot during ignition. In reference 1 the major problems reported by Conover were eliminated and a very consistent set of data was obtained. The techniques employed in reference 1 were used to obtain the data presented in this report.

The present work describes a series of tests directed toward the collection of qualitative and quantitative data documenting the

main characteristics of the flow in the head-end section of the ASRM. In particular, the following objectives were to be accomplished with the test program.

- 1) Obtain information on the igniter plume structure and shape and its interaction with the star grain geometry.
- 2) Determine the region of the igniter plume impingement on the side walls of the slots of the star grain section model.
- 3) Determine the flow field characteristics of the subsonic, recirculating flow within the slot.
- 4) Measure the heat transfer coefficients at several locations inside the slot.
- 5) Measure the velocity distribution in the star slot using an LDV system

The above objectives were to be accomplished using the following techniques:

- 1) Flow visualization.
- 2) Oil smears
- 3) Static pressure measurements
- 4) Heat transfer coefficient measurements
- 5) Velocity measurements

Experimental Apparatus

The test article used in this investigation was a one-tenth scale, cold flow model based on the geometry of the Space Shuttle RSRM head-end section. The test article had four slots, as opposed to eleven slots in the actual Space Shuttle motor. Two igniter models were tested. The first model had a centerport nozzle and four (4) nozzles canted at an angle of 22.5 degrees from the centerline of the igniter. The second igniter model was different in that the cant angle of the four (4) canted nozzles was 45.0 degrees. The nozzle dimensions were sized to provide the same mass flow rate as the nozzles previously studied in reference 1.

The scale factor of 1:10 was derived from an analysis which matches the Reynolds number between the model flow and the full scale flow in the star grain section. Besides geometrical similitude, the primary scaling parameter to ensure proper similarity between the cold flow model and the real, full scale

motor is the Reynolds number. Compressibility effects are important only in the igniter plume region, since the flow inside a star slot is essentially subsonic. However, the igniter mass flow rate is an important parameter, since it is thought to be responsible for entrainment of the flow, which determines the recirculation pattern. The value of the Reynolds number determines the nature of the viscous effects. The viscous effects in turn are related to the local convective heat transfer coefficient and therefore to the amount of heat transfer from the hot gases to the solid propellant. An exact match of Reynolds number between the model and full scale flow field is not necessary for similarity. Instead, generally good agreement between Reynolds numbers is a sufficient condition for the general studies of these flow fields, as has been extensively documented in the literature.³⁻⁶ The details of the scaling procedure are given in reference 1. A schematic of the star slot and a typical cross section of the star slot region are shown Figures II-1 and II-2.

The number of slots was determined based on different criteria. According to the analysis in reference 1, the Reynolds number is independent of the number of slots. Therefore, one can ideally choose any convenient number. Even though the actual SRM head-end section has eleven slots, only four slots are used in the scaled model. This represents a tradeoff between the desirability of flow visualization in one (transparent) star slot and the requirements for all other test instrumentation.

The entire star grain section model, as well as the three igniter models, were fabricated from aluminum, except for the transparent slot which consists of two plexiglas plates. The total length of the model is 19.72 inches; the largest diameter is 16 inches. Figure II-3 shows a schematic representation of the entire model. Figure II-4 is a photograph of the head end model and also of the igniter model used in reference 1 and in the current work. The first three igniter model on the left were used in reference 1, while the remaining two models were used in the present study.

Each star slot is formed from two plates separated by a bottom spacer of suitable thickness. An insert at the head-end simulates the actual grain surface. The circular port is formed from four contoured pieces connected to the outer surface of the slot plates. Two plates are located at the upstream and downstream end to close the slots, and provide the attachment points for all the parts. The igniter is connected to the inner surface of the head-end plate. The model is fully instrumented for measuring the parameters of interest as defined above.

Static pressure measurements are taken inside a single star slot and along two of the four contoured sectors forming the circular port of the model. Three pressure ports are located along each of the two contoured sectors. Twenty-eight static pressure ports are provided in one wall of a star slot. The measurements

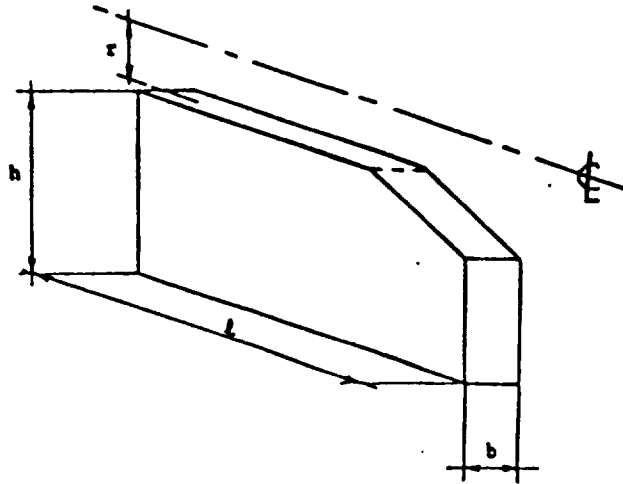


Fig. II-1 Schematic of star slot

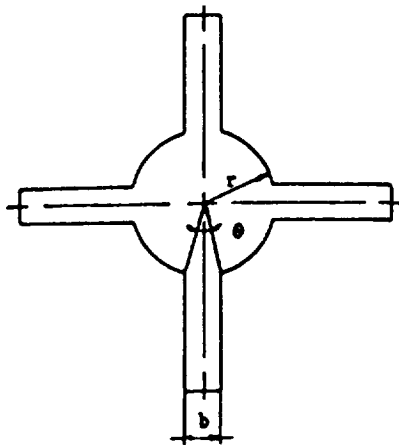


Fig. II-2 Cross-section of star slot region

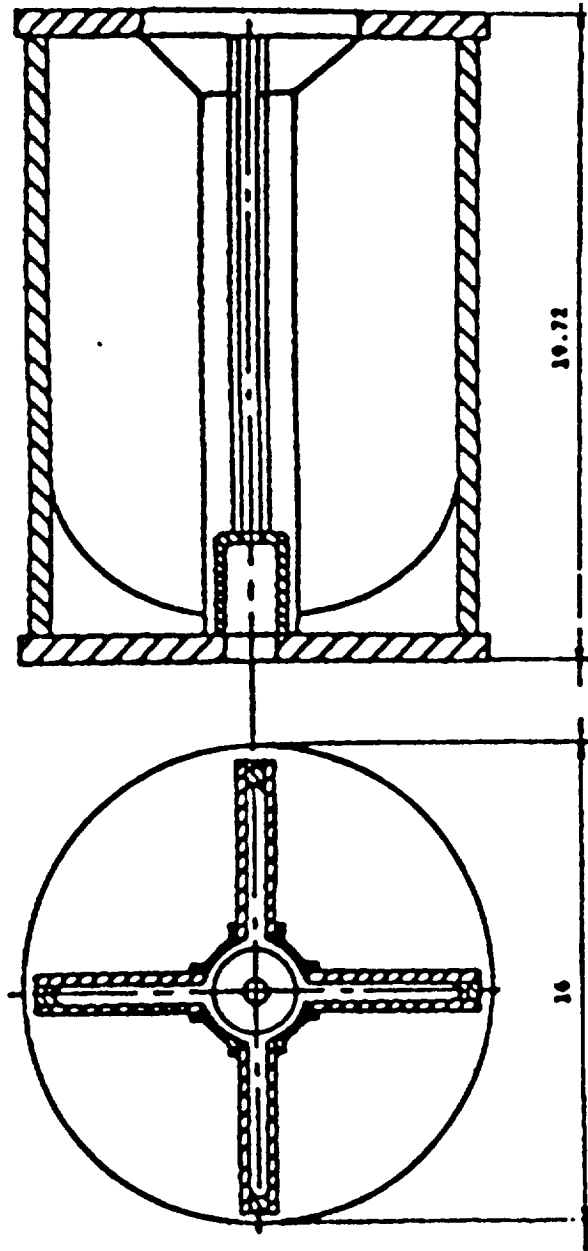


Figure II-3. Schematic of head-end section

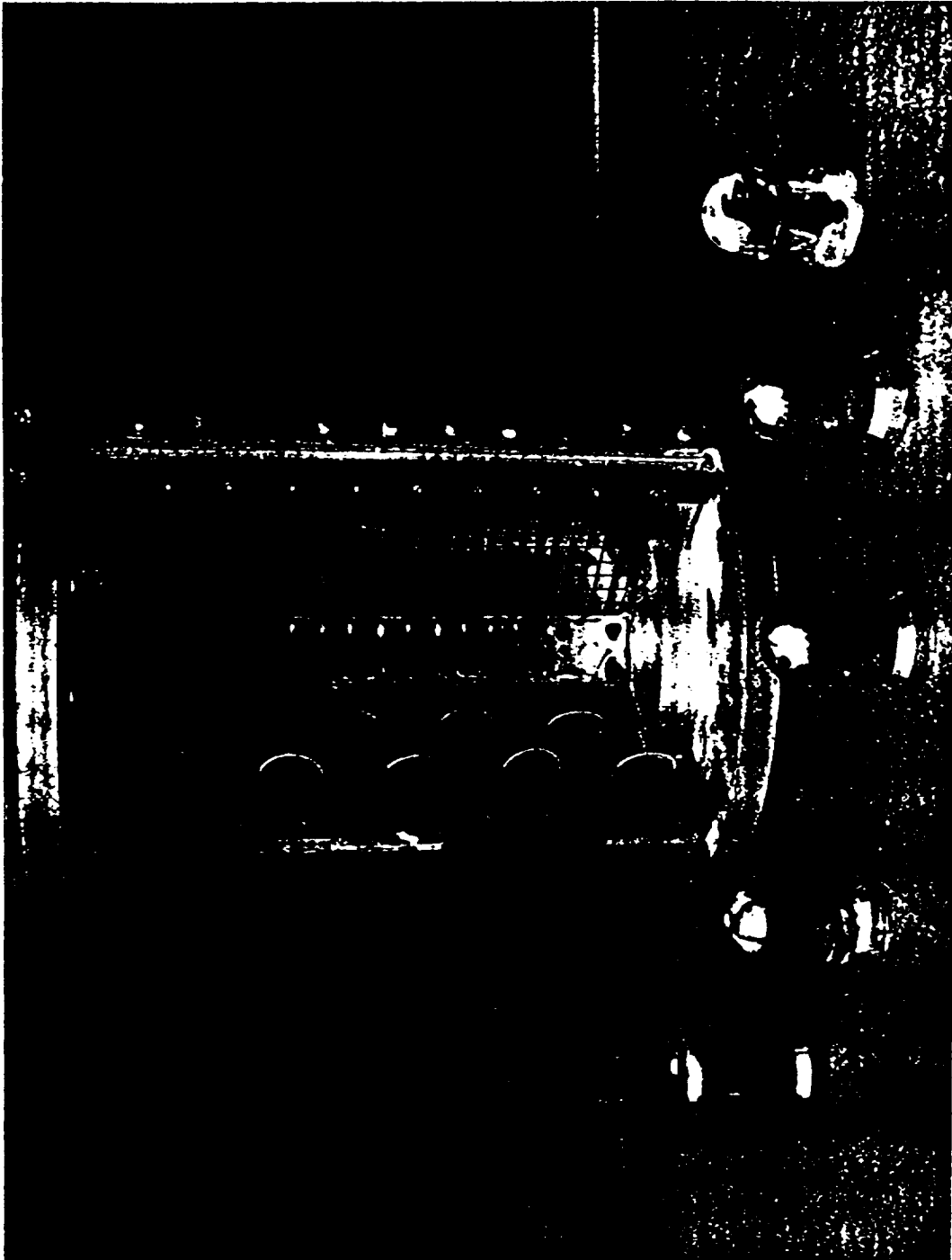


Figure II-4. Head-end slots and igniter models

are taken at three different slot depths and consist of eight, ten, and eight pressure taps, respectively, as shown in Fig. II-5. The three depths are equally spaced along the height of the slot.

In the plate forming the wall adjacent to the one containing the pressure taps, twenty-eight calorimeters are installed to obtain heat transfer coefficient data. A detail of the calorimeter installation is given in Fig. II-6. The calorimeters are placed at the same geometric locations as the pressure ports (Fig. II-5). Each calorimeter is mounted in a plug, flush with the inner surface of the slot plate. In order to get accurate measurements of the heat transfer coefficients, the calorimeters were pre-heated before each measurement was taken.

A second star slot was used to obtain oil smear data. A silicone-based oil was used to apply a matrix of oil drops to the finished surface of one of the plates in the slot. After each run, well defined marks or smears indicated the local direction of the flow and gave a good overall picture of the flow field.

The transparent slot previously mentioned was used for real time flow visualization. A laser sheet was projected from the aft-end of the model and illuminated most of the transparent slot. Aluminum particles mixed with pure alcohol were injected into the slot and the aluminum particles were illuminated by the laser sheet. The movement of the particles was clearly visible in the transparent slot and provided an excellent qualitative measurement of the behavior of the flow field in the slot. The flow visualization obtained using the aluminum particles gave a more detailed picture of the flow patterns in the slot than was possible with the oil smears. In addition, the real time nature of measurements provided a means for studying the dynamic characteristics of the flow field. Video tape recordings of these experiments were made to document the measurements.

Test Facility

The cold-flow tests used the special test section in the NASA Marshall Space Flight Center 14x14-inch trisonic wind tunnel. The tunnel operated as an intermittent blow-down wind tunnel from storage pressure to atmospheric exhaust. The full Mach number capability was not needed for the test program which was carried out. Instead only a high pressure internal flow through the special test section was required. The high pressure air passed through the hollow centerbody of the special test section, into a

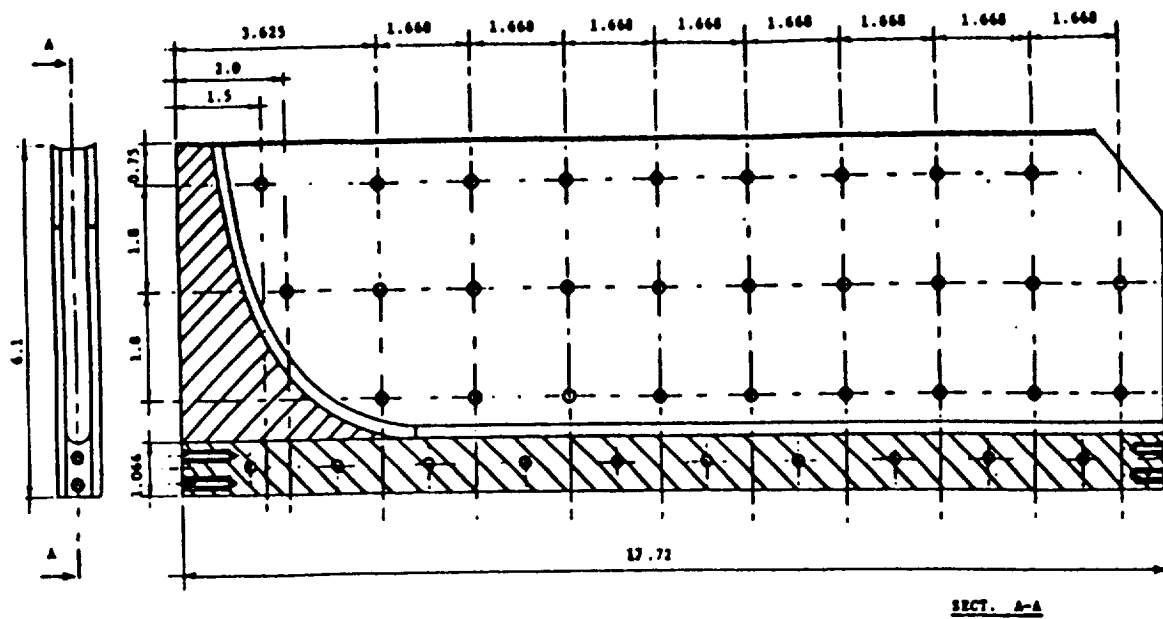


Figure II-5. Location of pressure taps and calorimeters

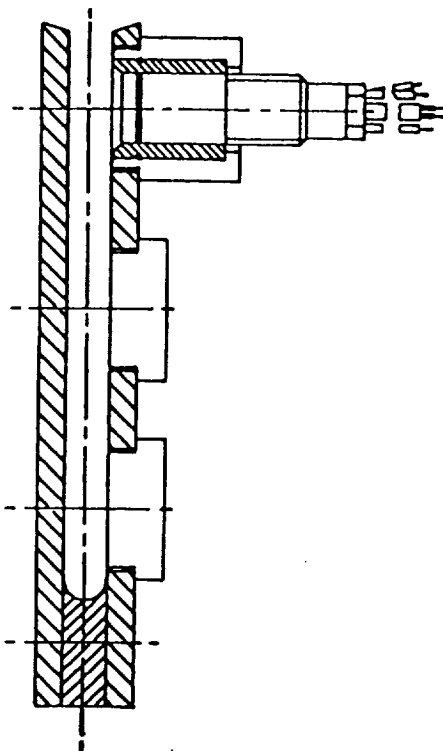


Figure II-6. Detail of calorimeter installation

pipe connected to the head-end plate of the model. It was then exhausted into the special test section through the igniter models. There was no external flow around the model. A venturi was installed upstream of the model to determine the mass flow rate through the igniter. Additional information regarding the NASA/MSFC trisonic wind tunnel is given in Ref. 7.

Test Plan

The test program included two main series of tests. Table II-1 shows the test matrix which was used for each series of tests. In the first series each igniter model was placed in the test section without the star grain portion of the model. Air flow at pressures of 100, 500, 1000, 1500 and 1800 psi passed through each of the igniters used in the experiments and mass flow rates corresponding to each pressure were recorded. A Schlieren system and video tape recorder were used during each run to examine the plume shape at various pressures. This was done to establish a reference for the plume geometry which could be compared with the plume geometry observed with the star grain in place. Photographs of the plume shapes for the two igniters at chamber pressures of approximately 100 psi and 1800 psi are shown in Figure II-7 through II-10 respectively.

The second series of tests used the entire head-end section model along with each of the three igniters. Oil smear, flow visualization, static pressure and heat transfer coefficient measurements were made at each condition shown in the test matrix of Table II-1. It should be noted that the test condition at 1800 psi approximates the design condition of 2000 psi at which similitude between the one-tenth scale model and the actual flow field is achieved. The value of 1800 psi was used because it represents the upper limit on the facility at the mass flow rates necessary for the tests.

Table II-1. Test matrix

Igniter Angle (deg)	Chamber Pressure (psi)	100	500	1000	1500	1800
22.5		1	2	3	4	5
45		6	7	8	9	10

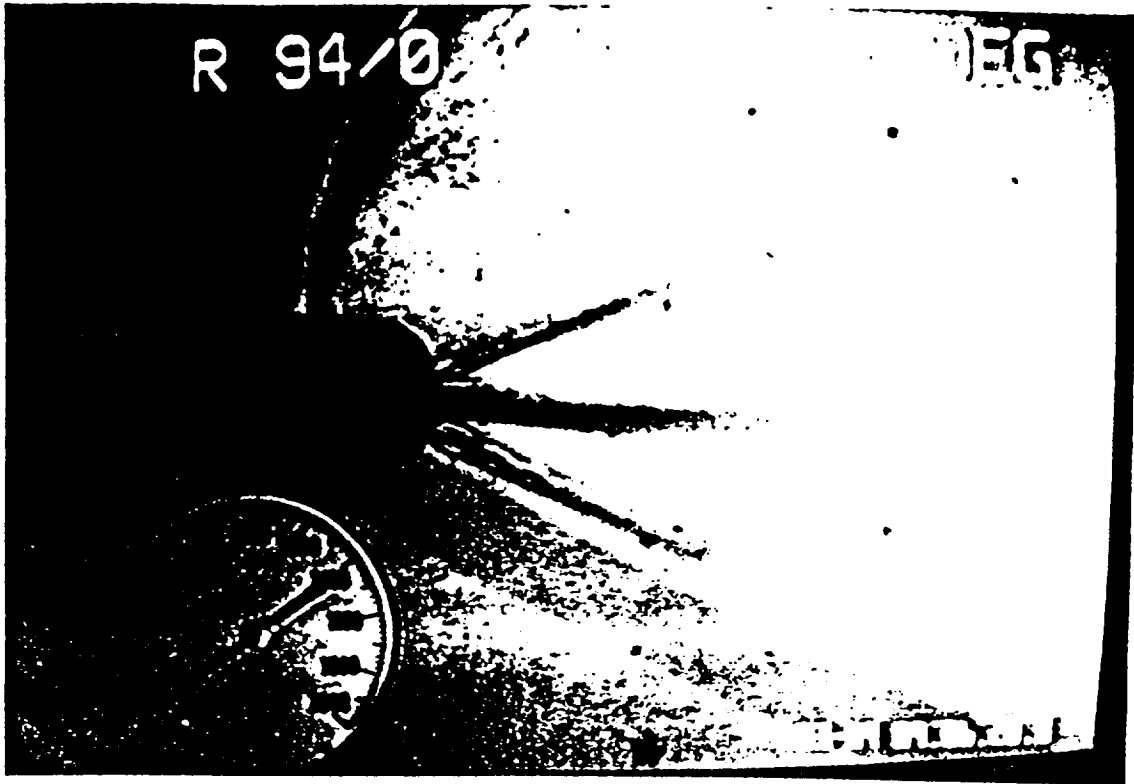


Figure II-7. Igniter 4 (100 psi)

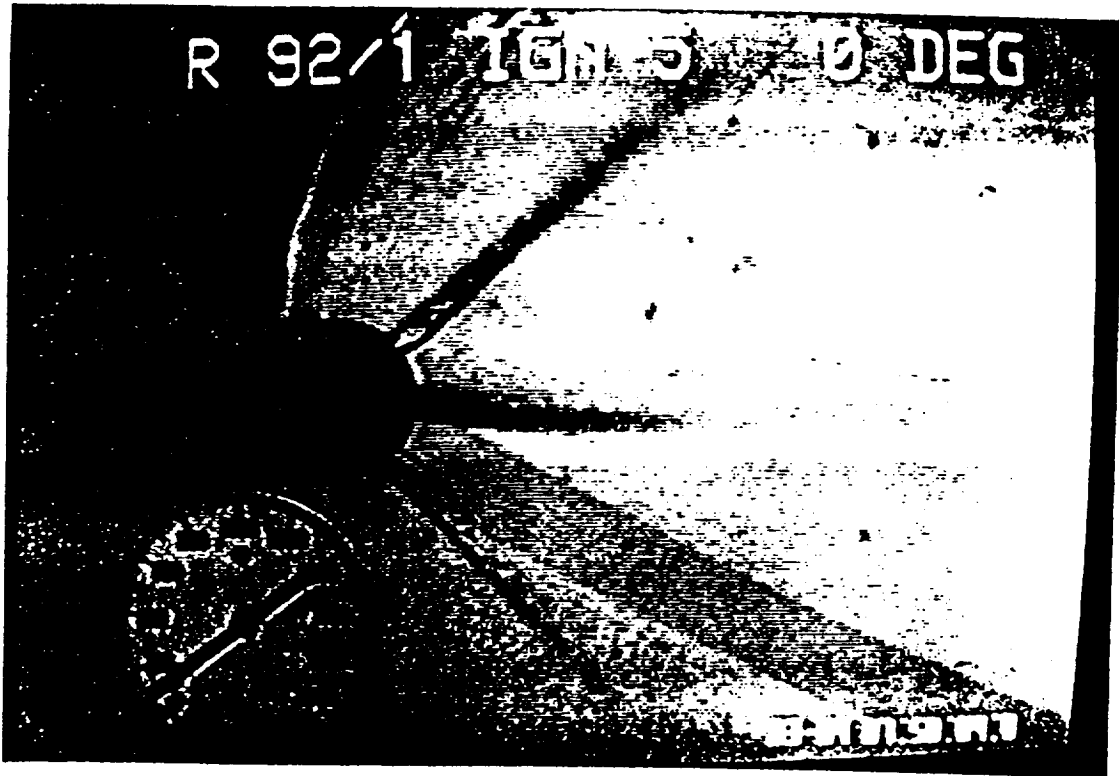


Figure II-8. Igniter 5 (100 psi)

II-10

ORIGINAL PAGE IS
OF POOR QUALITY

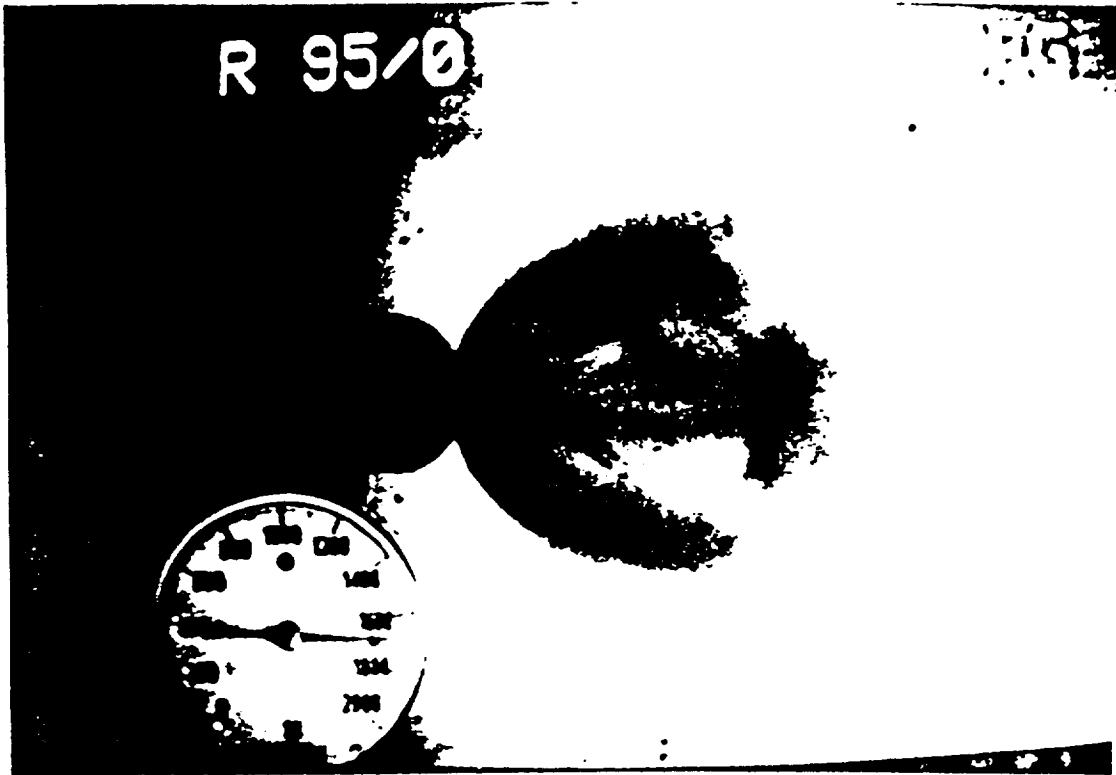


Figure II-9. Igniter 4 (1800 psi)

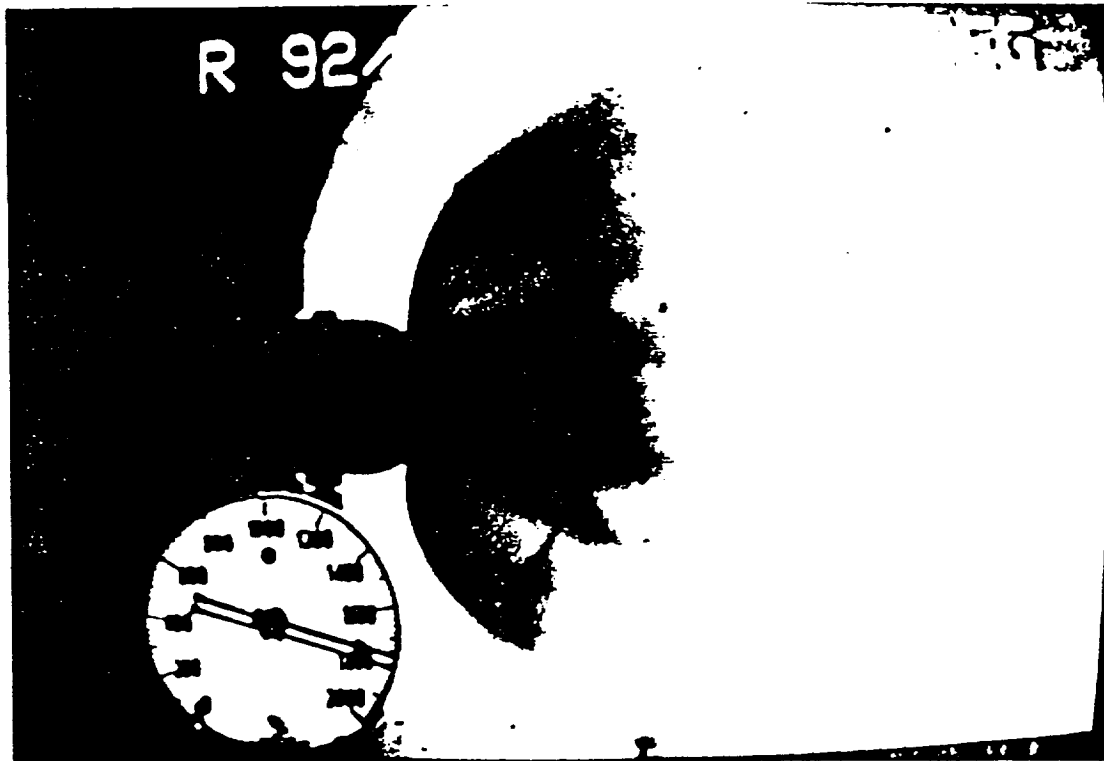


Figure II-10. Igniter 5 (1800 psi)

Oil Smear Test Results

Oil smears were taken for each of the fifteen test conditions shown in Table II-1. The oil smears were generated from a pattern of oil droplets placed on one side of a slot. The spacing between the droplets was approximately one-half inch. Figs. II-11 through II-20 show photographs of the oil smears generated for each of the 10 test conditions. The oil smears provide considerable detail regarding the direction of the primary flow in the slots, the region of the igniter plume impingement, and the recirculation patterns which occur in the slot. Although qualitative in nature, this data showed good agreement with the data from the CFD analyses presented in references 7-9.

Results From Static Pressure Measurements

Static pressure measurements were made at 27 locations on the surface of one of the slots. Fig. II-7 shows the location and numbering scheme used for the static pressure ports. Static pressure distributions obtained from these measurements are shown in Figs. II-21 through II-30. This data confirms the quantitative data obtained from the oil smear tests with regard to the location of the main flow paths, recirculation regions, stagnation points and "dead" regions within the slot.

Results From Heat Transfer Measurements

Calorimeters were placed in a slot face adjacent to the slot face where the static pressure measurements were made. The calorimeters were located at points corresponding to the 27 locations shown in Fig. II-7. Because of the lack of a sufficient number of calorimeters to measure data at all 27 locations simultaneously, two runs were made using 15 calorimeters in each run. Three calorimeters were not moved between runs to insure that consistent data were being obtained between the two runs. The results for the measured heat transfer coefficients are shown in Figs. II-31 through II-40.

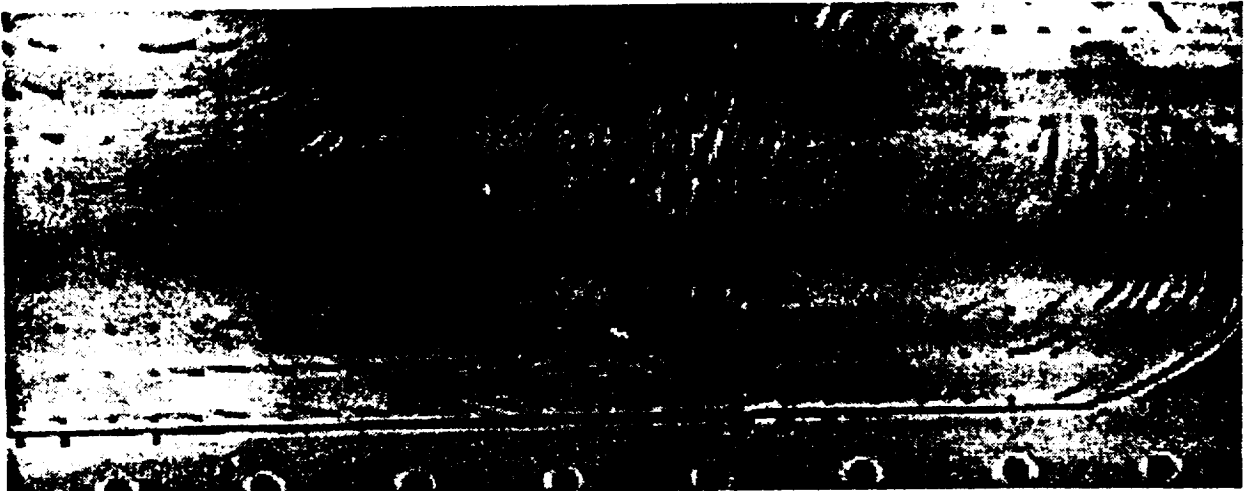


Figure II-11. Igniter 4 (100 psi)

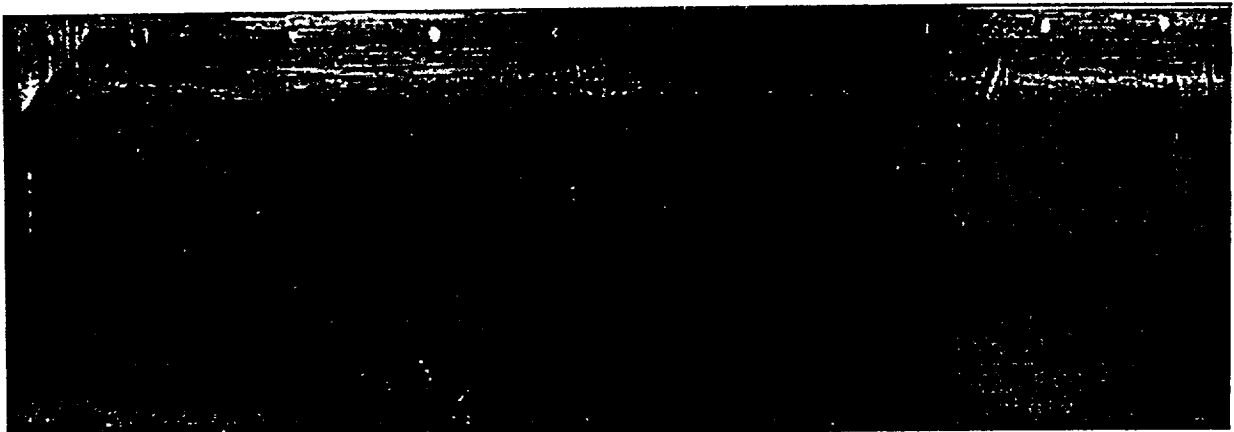


Figure II-12. Igniter 5 (100 psi)

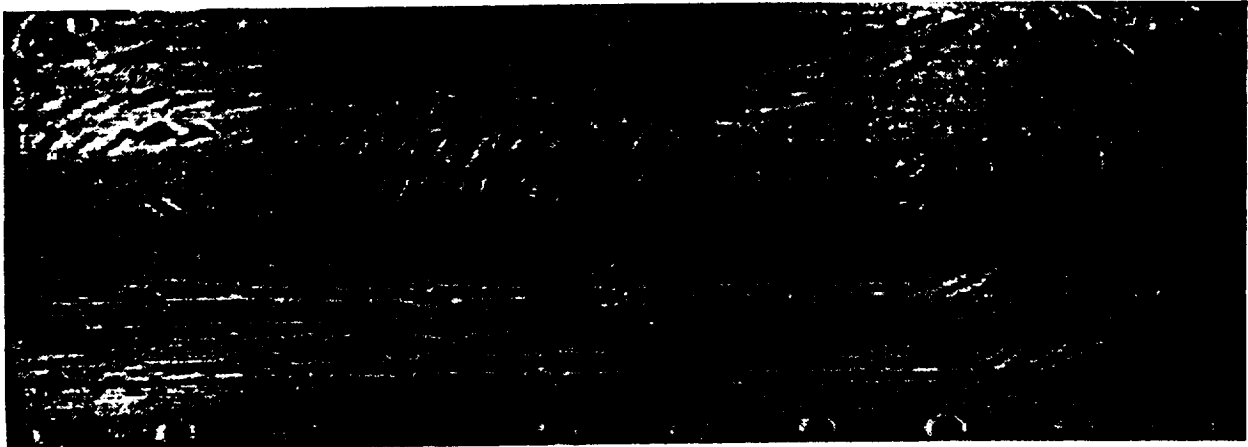


Figure II-13. Igniter 4 (500 psi)

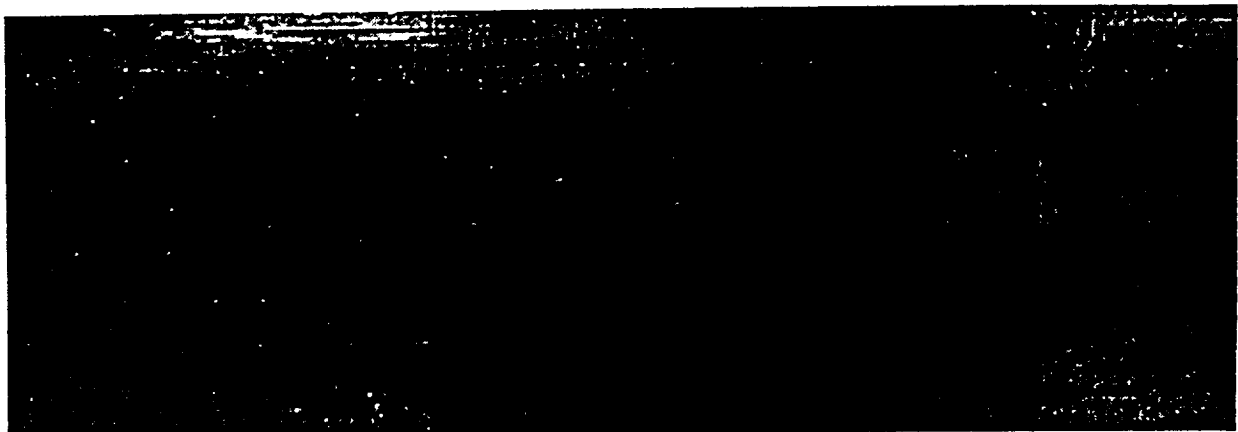


Figure II-14. Igniter 5 (500 psi)

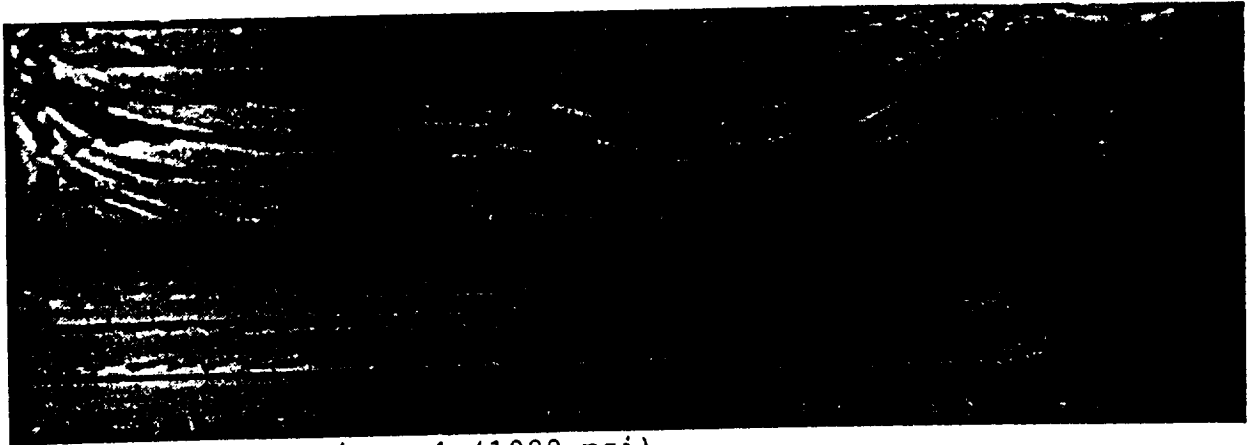


Figure I-15. Igniter 4 (1000 psi)

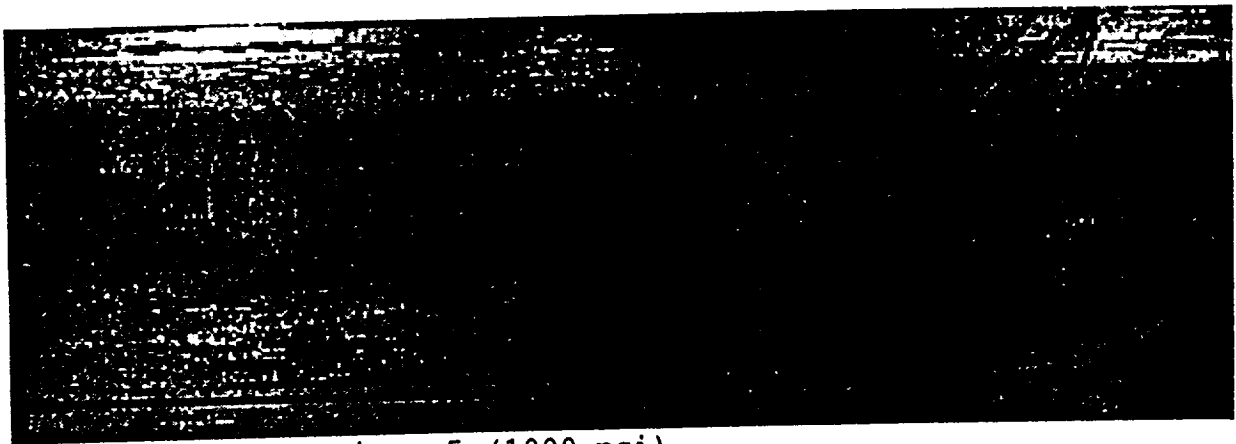


Figure II-16. Igniter 5 (1000 psi)

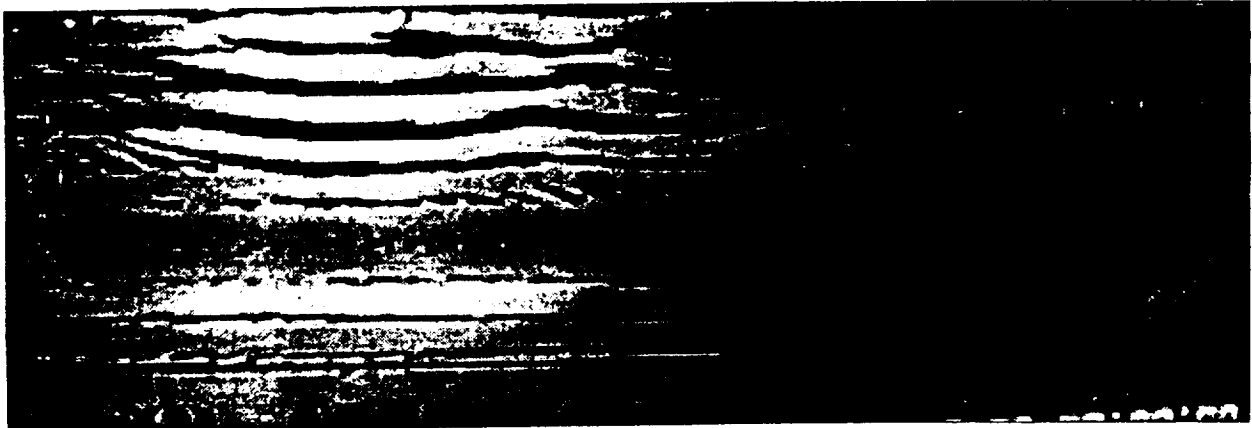


Figure II-17. Igniter 4 (1500 psi)

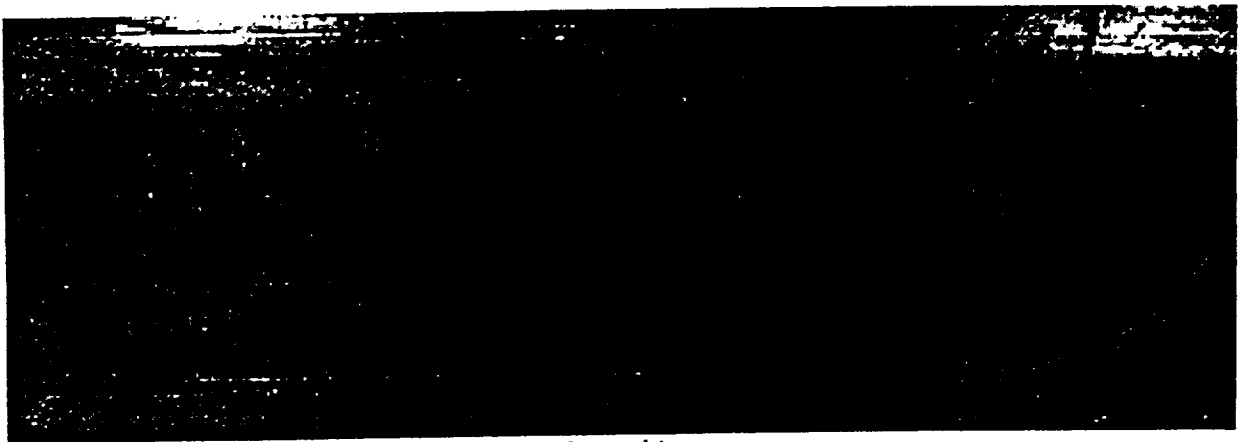


Figure II-18. Igniter 5 (1500 psi)



Figure II-19. Igniter 4 (1800 psi)

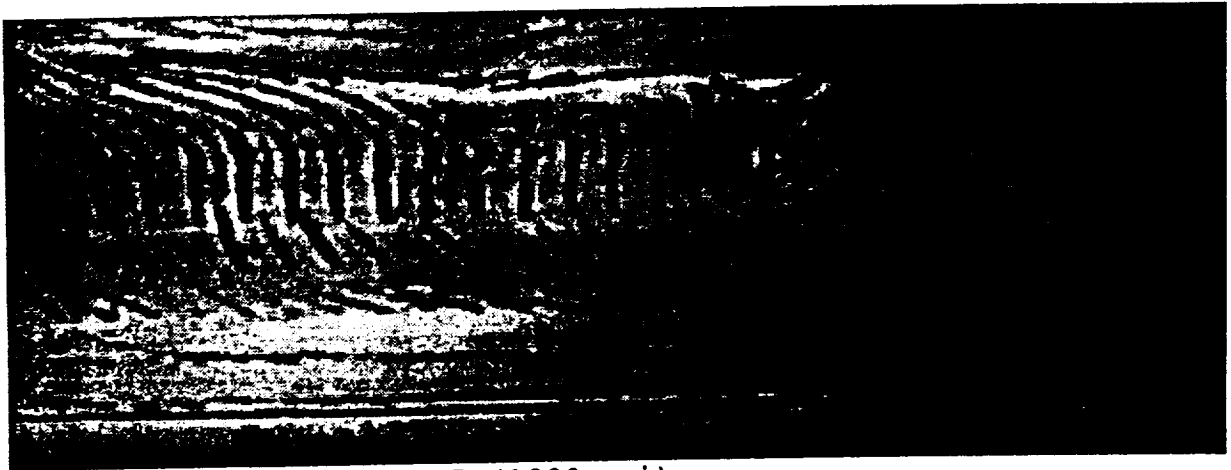


Figure II-20. Igniter 5 (1800 psi)

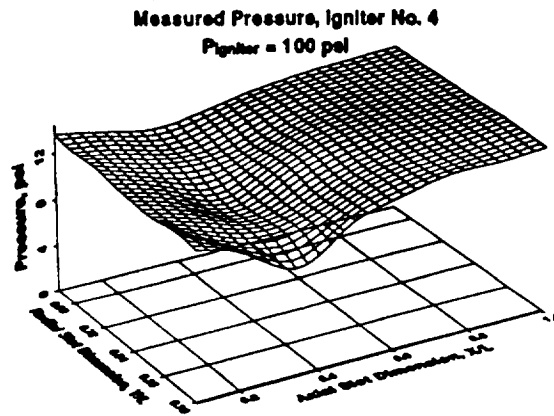


Figure II-21. Igniter 4 (100 psi)

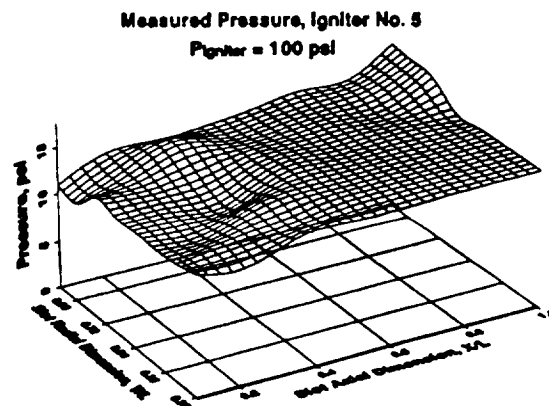


Figure II-22. Igniter 5 (100 psi)

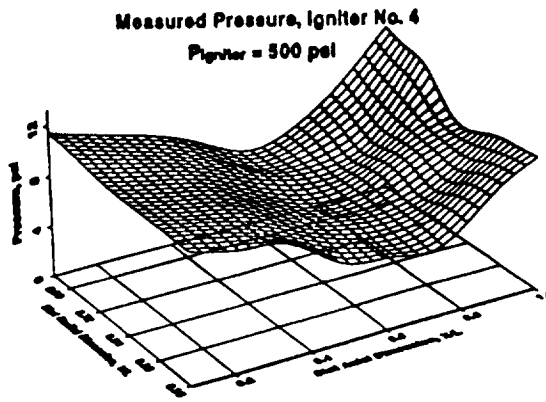


Figure II-23. Igniter 4 (500 psi)

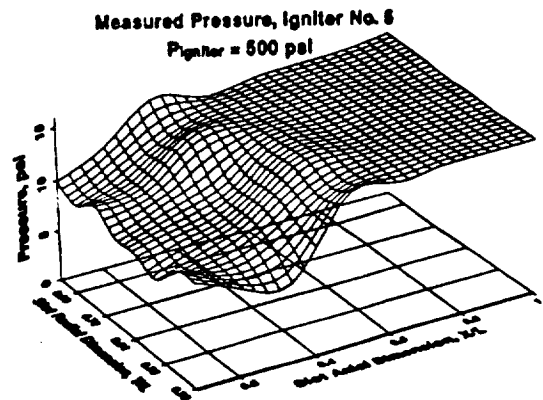


Figure II-24. Igniter 5 (500 psi)
 II-19

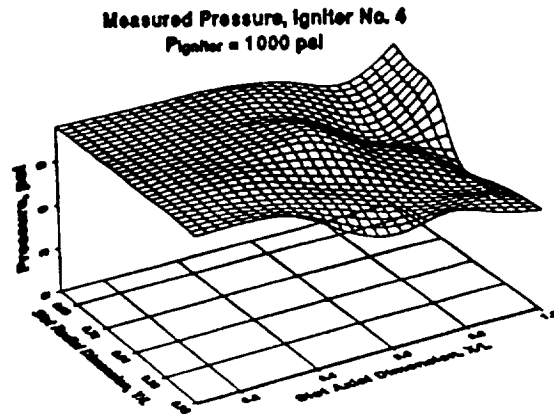


Figure II-25. Igniter 4 (1000 psi)

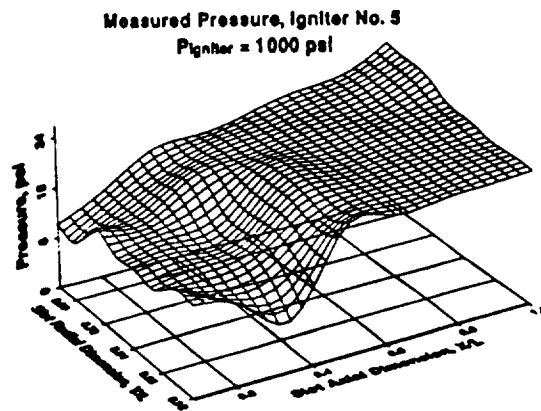


Figure II-26. Igniter 5 (1000 psi)

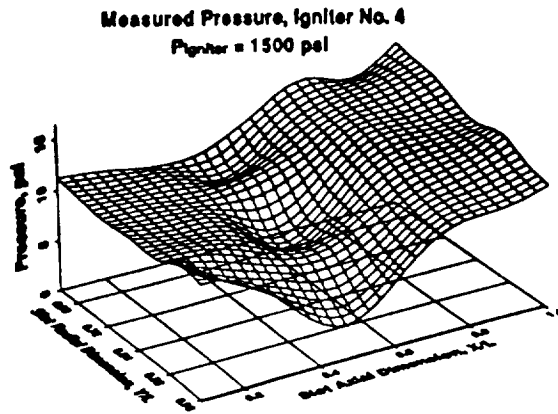


Figure II-27. Igniter 4 (1500 psi)

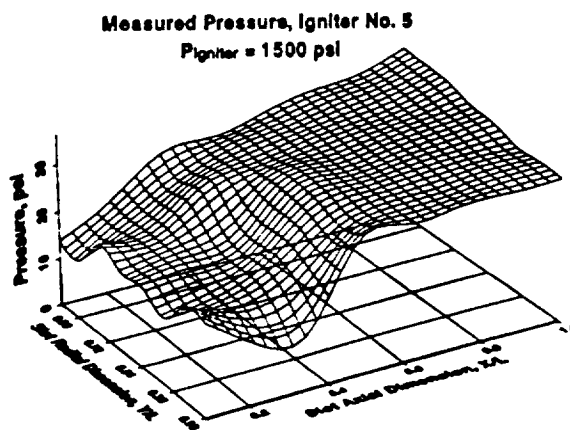


Figure II-28. Igniter 5 (1500 psi)

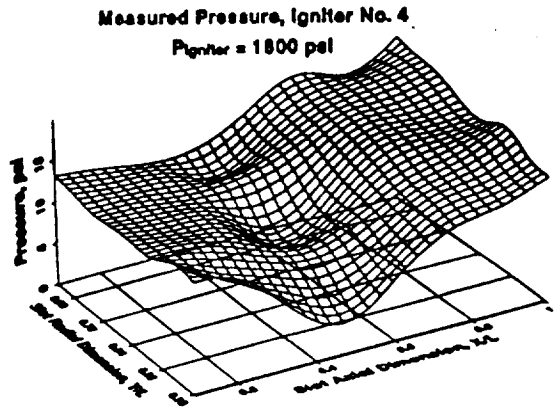


Figure II-29. Igniter 4 (1800 psi)

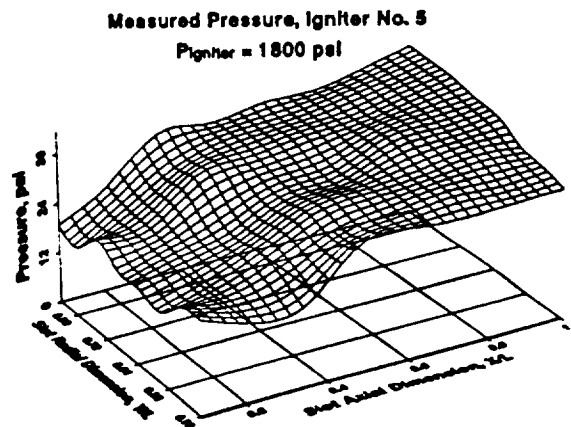


Figure II-30. Igniter 5 (1800 psi)
II-22

Measured Heat Transfer, Igniter No. 4
P_{igniter} = 100 psi

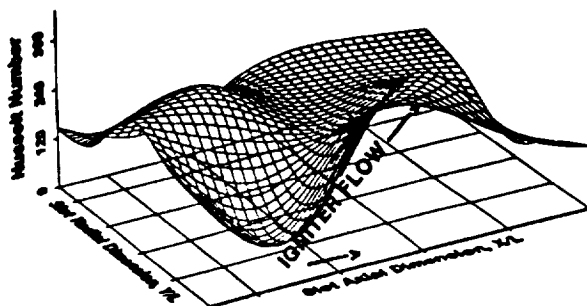


Figure II-31. Igniter 4 (100 psi)

Measured Heat Transfer, Igniter No. 5
P_{igniter} = 100 psi

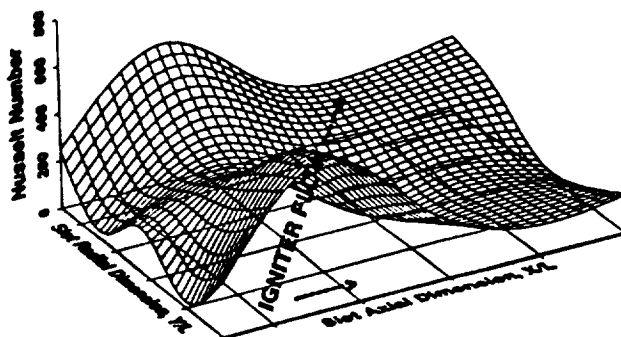


Figure II-32. Igniter 5 (100 psi)

Measured Heat Transfer, Igniter No. 4
P_{igniter} = 500 psi

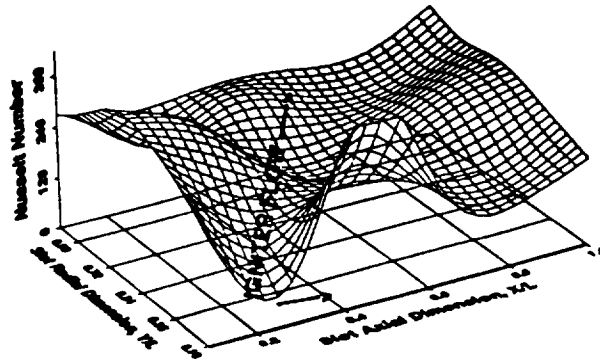


Figure II-33. Igniter 4 (500 psi)

Measured Heat Transfer, Igniter No. 5
P_{igniter} = 500 psi

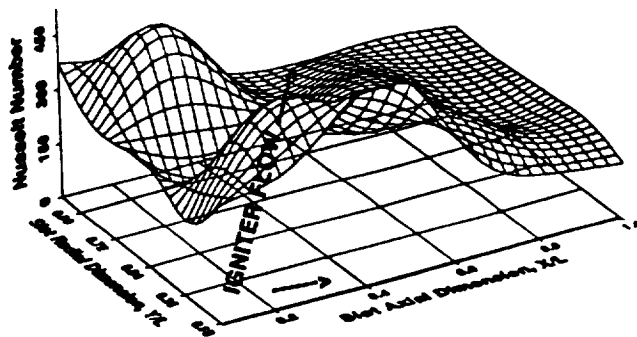


Figure II-34. Igniter 5 (500 psi)

Measured Heat Transfer, Igniter No. 4
P_{igniter} = 1000 psi

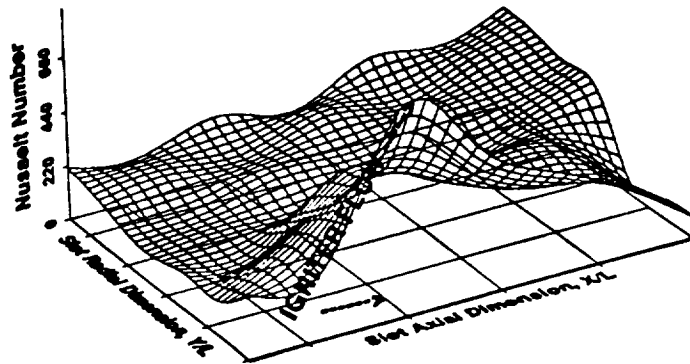


Figure II-35. Igniter 4 (1000 psi)

Measured Heat Transfer, Igniter No. 5
P_{igniter} = 1000 psi

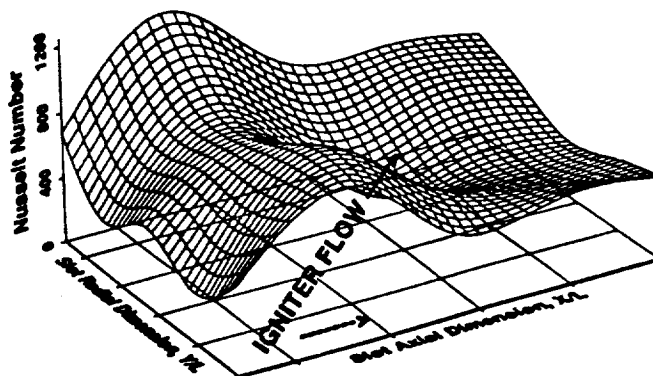


Figure II-36. Igniter 5 (1000 psi)
II-25

Measured Heat Transfer, Igniter No. 4
P_{igniter} = 1500 psi

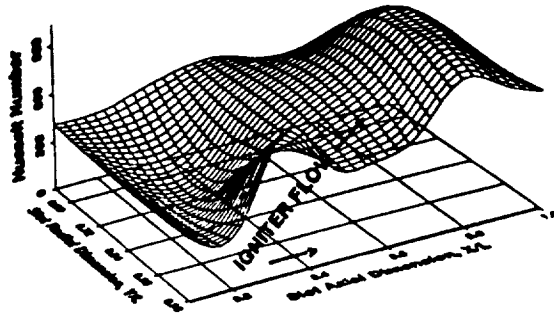


Figure II-37. Igniter 4 (1500 psi)

Measured Heat Transfer, Igniter No. 5
P_{igniter} = 1500 psi

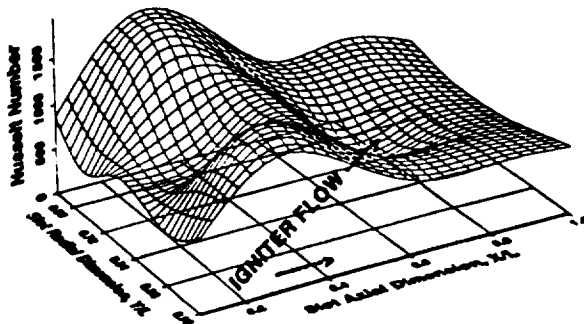


Figure II-38. Igniter 5 (1500 psi)

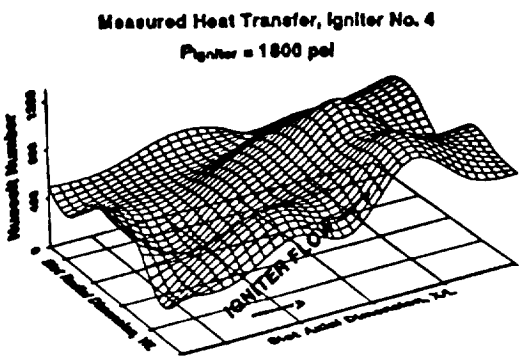


Figure II-39. Igniter 4 (1800 psi)

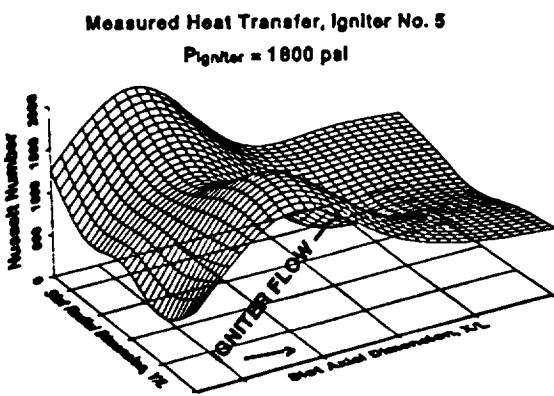


Figure II-40. Igniter 5 (1800 psi)

LDV Experiment

It was desired to make direct velocity measurements inside the star slot. The use of hot wire anemometry was previously ruled out, because of the flow obstruction and the inability of the probes to survive in the supersonic region of the flow field. The cost of converting the plexiglas panels to optical glass panels which were present in one slot was prohibitive. Therefore, it was decided to modify the existing calorimeter ports to accept a fitting containing an optical window. This window would then be used to provide access to the flow field with the laser at the discrete positions where the calorimeters and pressure ports were located. A photograph of the experimental setup, showing the laser and the optical window, is shown Figure II-41. The flow was seeded using an alcohol and aluminum particle mixture which could be illuminated by the laser and thus the LDV system could then be used to measure the local velocity components. The LDV system used was capable of measuring two components of velocity in the plane of the star slot. A photograph of the LDV system in operation is shown in Figure II-42. The optical view-port was then moved to different locations to obtain a map of the velocity field inside the slot as a function of igniter chamber pressure.

The seeding was accomplished by injecting the mixture of alcohol and aluminum particles into the flow field near the exit plane of the igniter model nozzle. For purposes of comparison two igniter models were used in this experiment. They were the 22.5 degree, four port igniter without a centerport and the 45 degree igniter with a centerport. The angle indicates the cant angle of the igniter ports with respect to the centerline of the model. A photograph of the igniter models used in the LDV experiment are shown in Figure II-43.

Preliminary calculations indicate that the measured velocity components were near those that would be predicted from the pressure distribution data. At present these data are being studied and will be documented in a paper which will serve as an addendum to this report.

Although extensive video was taken through the plexiglas slots, no still photos were taken of the circulation patterns within the slot. However, when the flow was seeded, the aluminum particles tended to adhere to the plexiglas plates. The pattern of aluminum particles on the plexiglas provided an illustration of the type of circulation present in the star slots. A typical photograph of this phenomena is shown in Figure II-44.



Figure II-41. LDV experimental setup

ORIGINALLY PREPARED BY
DIA PROGRAM CONTROL DIVISION

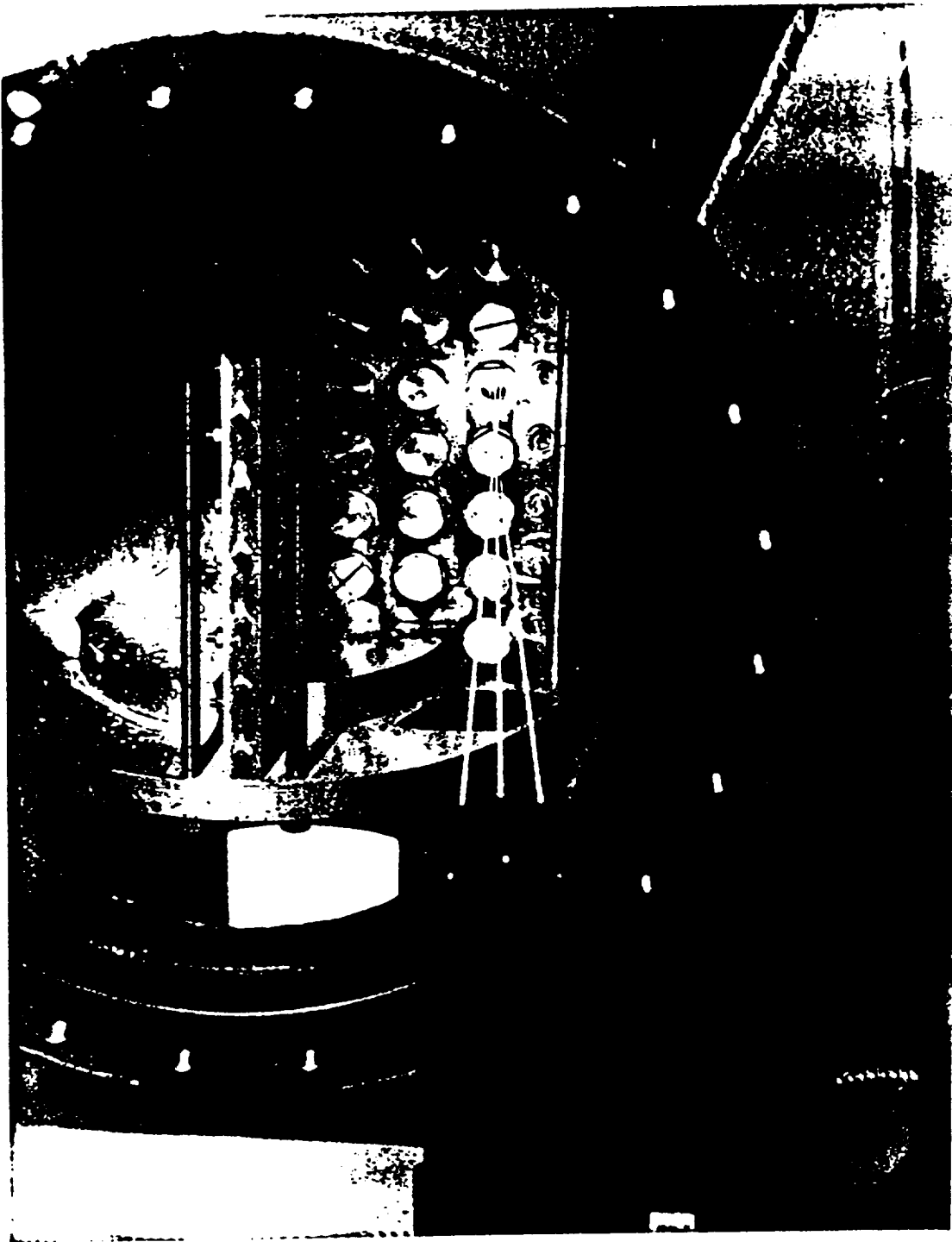


Figure II-42. LDV system in operation

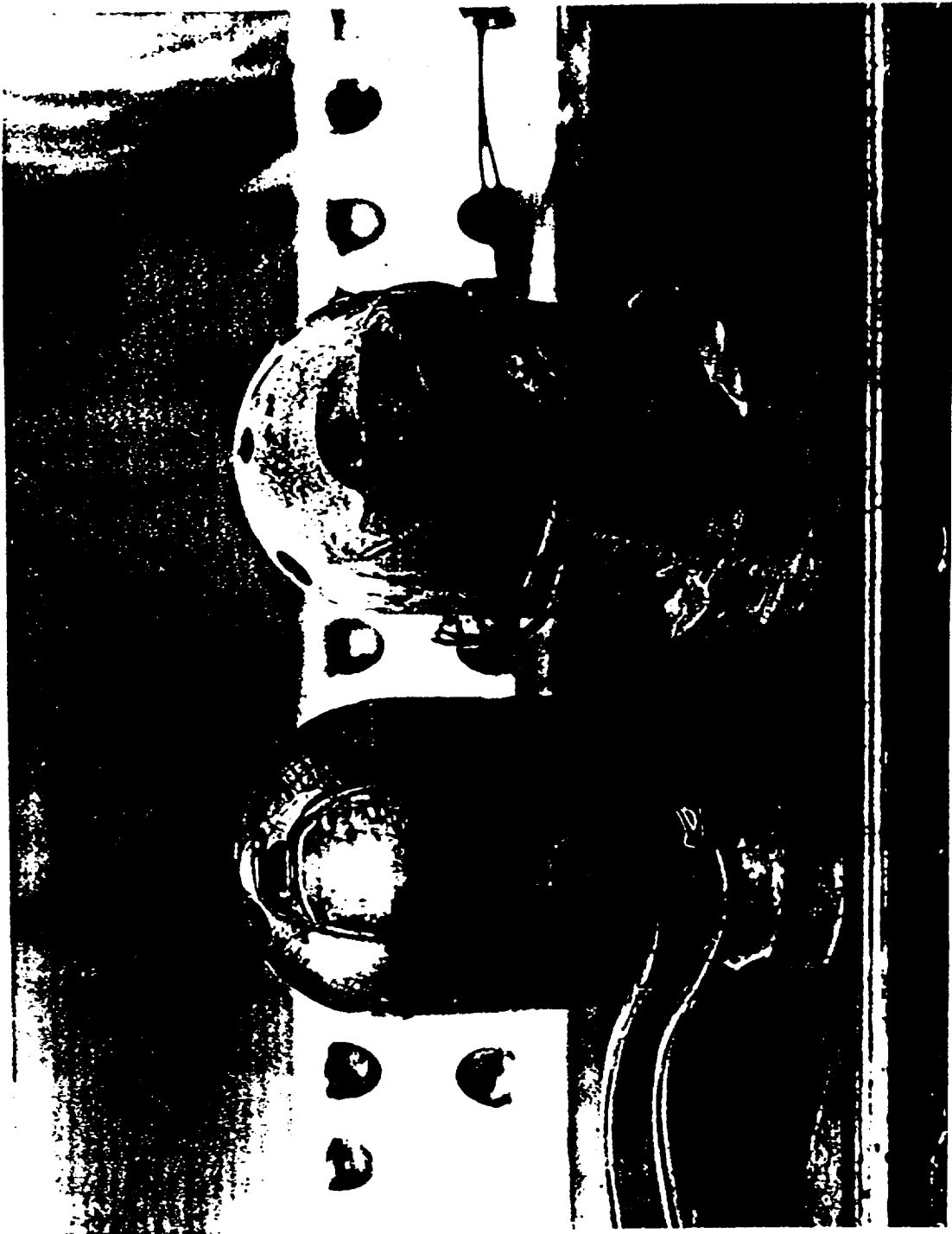


Figure II-43. Igniter models used for LDV measurements

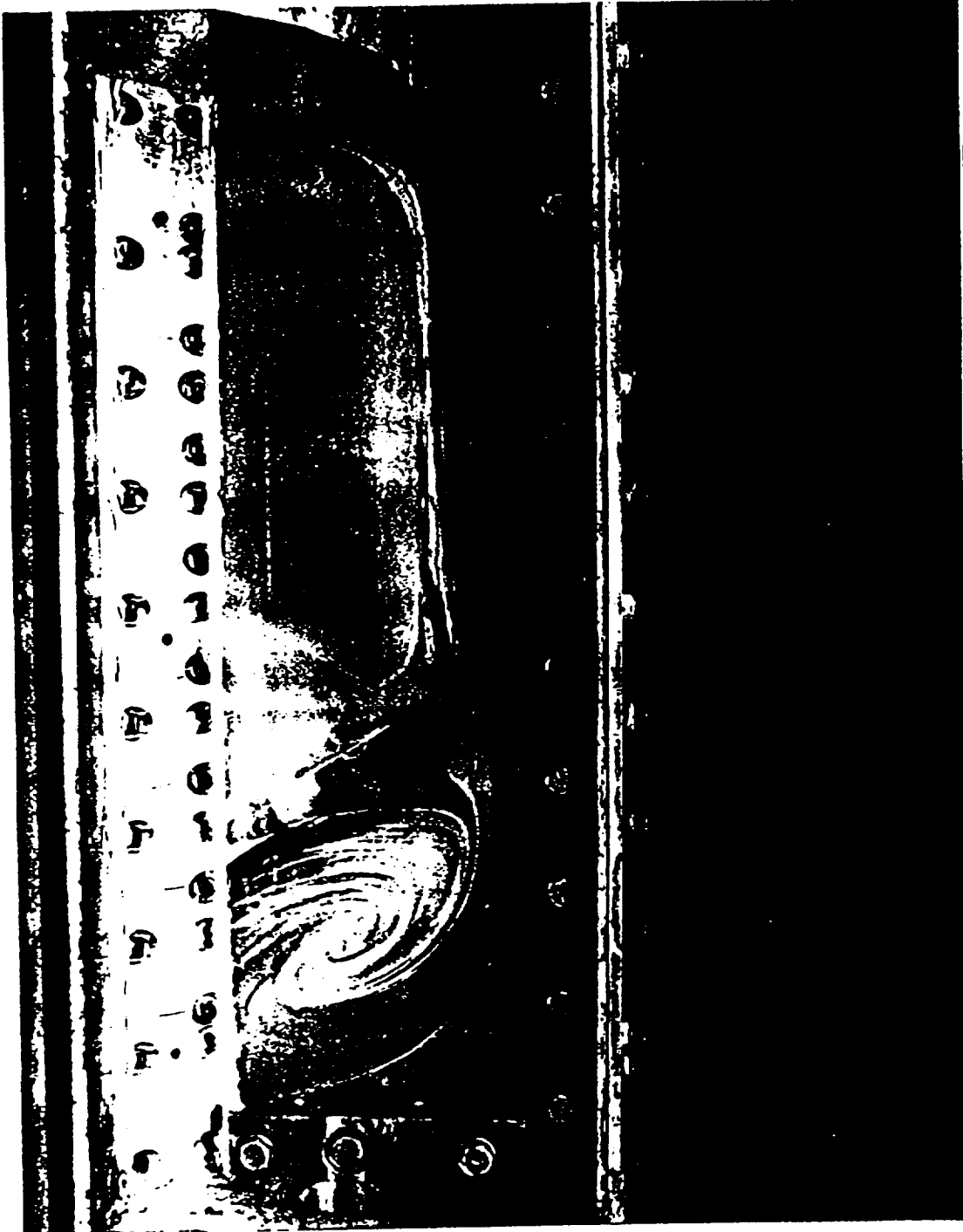


Figure II-44. Etching formed by Al particles on plexiglas slot

References

1. Foster, W. A., Jr., Jenkins, R. M., Ciucci, A. and Johnson, S. D., "Development of a New Generation Solid Rocket Motor Ignition Computer Code," Final Report, NASA Grant No. NAG8-683, Auburn University, February, 1994.
2. Conover, G. H., Jr., "Cold-Flow Studies of Igniter Plume Flow Fields and Heat Transfer," Final Report, NASA Grant No. NGT-01-003-800, Auburn University, June 1984.
3. Schetz, J. A., Hewitt, P. A., and Thomas, R., "Swirl Combustion Flow-Visualization Studies in a Water-Tunnel," Journal of Spacecraft and Rockets, Vol. 20, No. 6, Nov-Dec., 1983, pp.574-582.
4. Schetz, J. A., Guruswamy, J., and Marchman, J. F., III, "Effects of an S-Inlet on the Flow in a Dump Combustor," Journal of Spacecraft and Rockets, March-April, 1985, pp. 221-224.
5. Schetz, J. A., Sebba, F., and Thomas, R. H., "Flow-Visualization Studies of a Solid Fuel Ramjet Combustor Using A New Material-Polyaphrone," 22nd Joint Army, Navy, NASA, Air Force Combustion Meeting, October, 1985.
6. Caveny, L. H., and Kuo, K. K., "Ignition Transients of Large Segmented Rocket Boosters," April 1976, NASA Contractor Report CR-1501162, NASA George C. Marshall Space Flight Center.
7. Simon, E., "The George C. Marshall Space Flight Center's 14x14-Inch Trisonic Wind Tunnel Technical Handbook," NASA TMX-53185, December, 1964.